View metadata, citation and similar papers at core.ac.uk

brought to you by CORE

provided by univOAK

Investigation of size effects on the structure of liquid $GeSe_2$ calculated via first-principles molecular dynamics

Matthieu Micoulaut, Sébastien Le Roux, and Carlo Massobrio

Citation: The Journal of Chemical Physics **136**, 224504 (2012); doi: 10.1063/1.4722101

View online: https://doi.org/10.1063/1.4722101

View Table of Contents: http://aip.scitation.org/toc/jcp/136/22

Published by the American Institute of Physics

Articles you may be interested in

Origin of structural analogies and differences between the atomic structures of $GeSe_4$ and GeS_4 glasses: A first principles study
The Journal of Chemical Physics **143**, 034504 (2015); 10.1063/1.4926830

The structure of liquid GeSe revisited: A first principles molecular dynamics study
The Journal of Chemical Physics **138**, 174505 (2013); 10.1063/1.4803115

Note: Accounting for pressure effects on the calculated equilibrium structure of glassy $GeSe_2$
The Journal of Chemical Physics **137**, 046101 (2012); 10.1063/1.4739953

Structure of amorphous $GeSe_9$ by neutron diffraction and first-principles molecular dynamics: Impact of trajectory sampling and size effects
The Journal of Chemical Physics **145**, 084502 (2016); 10.1063/1.4961265

Impact of dispersion forces on the atomic structure of a prototypical network-forming disordered system: The case of liquid $GeSe_2$
The Journal of Chemical Physics **147**, 044504 (2017); 10.1063/1.4986166

Structural study of $Na_2O–B_2O_3–SiO_2$ glasses from molecular simulations using a polarizable force field
The Journal of Chemical Physics **147**, 161711 (2017); 10.1063/1.4992799

PHYSICS TODAY
WHITEPAPERS

ADVANCED LIGHT CURE ADHESIVES

Take a closer look at what these environmentally friendly adhesive systems can do

READ NOW

PRESENTED BY
MASTERBOND
ADHESIVES | SEALANTS | COATINGS

Investigation of size effects on the structure of liquid $GeSe_2$ calculated via first-principles molecular dynamics

Matthieu Micoulaut,[1] Sébastien Le Roux,[2] and Carlo Massobrio[2]
[1]*Laboratoire de Physique Théorique de la Matière Condensée, Université Pierre et Marie Curie, 4 Place Jussieu, F-75252 Paris Cedex 05, France*
[2]*Institut de Physique et de Chimie des Matériaux de Strasbourg, 23 rue du Loess, BP43, F-67034 Strasbourg Cedex 2, France*

(Received 19 March 2012; accepted 10 May 2012; published online 11 June 2012)

The structural properties of liquid $GeSe_2$ have been calculated by first-principles molecular dynamics by using a periodic simulation box containing N = 480 atoms. This has allowed a comparison with previous results obtained on a smaller system size (N = 120) [M. Micoulaut, R. Vuilleumier, and C. Massobrio, Phys. Rev. B **79**, 214205 (2009)]. In the domain of first-principles molecular dynamics, we obtain an assessment of system size effects of unprecedented quality. Overall, no drastic differences are found between the two sets of results, confirming that N = 120 is a suitable size to achieve a realistic description of this prototypical disordered network. However, for N = 480, short range properties are characterized by an increase of chemical order, the number of Ge tetrahedra coordinated to four Se atoms being larger. At the intermediate range order level, size effect mostly modify the low wavevector region ($k \sim 1$ Å^{-1}) in the concentration-concentration partial structure factor. © *2012 American Institute of Physics*. [http://dx.doi.org/10.1063/1.4722101]

I. INTRODUCTION

The concomitant presence of a predominant structural unit (the $GeSe_4$ tetrahedron) and of homopolar bonds makes the atomic structure of liquid and glassy $GeSe_2$ challenging to elucidate for both experiments and atomic-scale modelling.[1–8] First-principles molecular dynamics based on density functional theory (DFT-FPMD in what follows), has shown that both short and intermediate range order of liquid and glassy $GeSe_2$ are extremely sensitive to the choice of a specific exchange-correlation (XC) functional.[9,10] In particular, GGA (generalized gradient approximated) functionals favoring electronic localization bring calculations in better agreement with structural data. Substantial improvements were found when introducing the Perdew-Wang (PW) recipe instead of the local density approximation (LDA) and, in a further step, the BLYP scheme (due to Becke for the exchange energy and to Lee, Yang, and Parr for the correlation energy) instead of the PW scheme.[9–14] By focusing on the case of liquid $GeSe_2$, it appears that partial structure factors obtained via DFT-FPMD are able to reproduce experimental data for an extended range of wavevectors in reciprocal space, the same consideration holding for pair correlation functions in real space.[4,10] However, a number of notable differences between theory and experiments do persist. The most elusive is the underestimate of the first sharp diffraction peak (FSDP) in the Ge-Ge partial structure factor, responsible for the absence of the FSDP in the Bhatia-Thornton concentration-concentration structure factor.[15] To date, available DFT-FPMD results on disordered Ge_xSe_{1-x} materials stem from the use of periodic simulation cells typically containing N = 120 atoms.[16–19] Based on recent achievements, it appears that statistical averages can be routinely taken on temporal trajectory lasting as much as 100 ps.[18] This situation withstanding, it is worthwhile to determine whether the use of a larger periodic simulation box has some impact on the predictive power of the available DFT-FPMD schemes. We stress that the possible occurrence of size-effects and anisotropies on periodic boundary *classical* molecular dynamics simulations has been the object of continuous interest.[20–35] Very large simulation boxes have been adopted to monitor the onset of such effects.[27–35] However, we are not aware of a DFT-FPMD study in which the results pertaining to two sizes of the simulation cell (of about 100 and 500 atoms) have been compared at the same level of statistical accuracy, i.e., by exploiting time trajectories of comparable lengths. This is exactly the purpose of our paper, devoted to the production of a new, complementary set of data on liquid $GeSe_2$, obtained with a periodic simulation cell containing N = 480 atoms. This work is organized as follows. Section II is devoted to the presentation of our model. Results on the partial structure factors are given in Sec. III. Real space properties (partial-pair correlation functions, coordination numbers, and bond-angle distribution) are given in Sec. IV. A brief account of the correlation with diffusion properties and the electronic behavior is contained in Sec. V. The paper ends with conclusive remarks (Sec. VI).

II. THEORETICAL MODEL

The theoretical framework of our calculations is identical to the one employed and detailed extensively in the past for N = 120.[4,10] In the present case, FPMD simulations have been performed at constant volume on a system containing 480 (160 Ge and 320 Se) atoms positioned in a periodically repeated cubic cell of size 24.89 Å, this value allowing to recover the experimental density of the liquid[36] at the desired temperature ($T = 1050$ K). We recall that the electronic structure was described within density functional theory (DFT)

 © 2012 American Institute of Physics

and evolved self-consistently in time.[37] A generalized gradient approximation was used, based on the exchange energy obtained by Becke,[12] and the correlation energy according to Lee, Yang, and Parr (BLYP).[13] Valence electrons have been treated explicitly, in conjunction with norm conserving pseudopotentials of the Trouiller-Martins type to account for core-valence interactions.[38] The wave functions have been expanded at the Γ point of the supercell on a plane wave basis set with an energy cutoff $E_c = 20$ Ry. In the first-principles molecular dynamics (FPMD) approach, a fictitious electron mass of 2000 a.u. (i.e., in units of $m_e a_0^2$ where m_e is the electron mass and a_0 is the Bohr radius), and a time step of $\Delta t = 0.12$ fs have been used to integrate the equations of motion. The control of the temperature has been implemented for both the ionic and electronic degrees of freedom by using Nosé-Hoover thermostats.[39–41] The initial coordinates of the 480 atoms system have been obtained by using a glassy configuration generated from a Mauro-Varshneya force field.[42] To lose memory of the initial configuration, simulations at $T = 2000$ K have been first carried out over a time period of 25 ps. The same length of time has been adopted to anneal further the system at the intermediate temperatures T = 1700 K and T = 1373 K. After discarding the first 25 ps at T = 1050 K, statistical averages have been collected over 63 ps, during which Ge and Se atoms have covered an average distance of 50 Å. It is worth pointing out that calculations performed on the N = 480 system turned out to be about 100 times more costly than the N = 120 system counterpart. This factor is in line with a computational effort that scales such as $\mathcal{O}$ ($N_s{}^2$MlnM) where N_s is the number of occupied orbitals and M is the number of basis functions (plane waves).[43] In what follows, a systematic comparison of the present results with the results obtained in Ref. 10 will be carried out. For both sets of calculations, statistical errors are limited to 5% at most.

III. STRUCTURE FACTORS

A. Partial structure factors

Bhatia-Thornton partial structure factors $S_{NN}(k)$ (number-number), $S_{NC}(k)$ (number-concentration), and $S_{CC}(k)$ (concentration-concentration) for liquid $GeSe_2$ are shown in Fig. 1 and compared to the results of Ref. 10 (N = 120) and to the experimental data of Ref. 1 obtained from isotopic substitution in neutron diffraction.

These can be obtained by linear combination of the Faber-Ziman partial structure factors $S^{FZ}_{GeGe}(k)$, $S^{FZ}_{SeSe}(k)$, and $S^{FZ}_{GeSe}(k)$ as follows:

$$S_{NN}(k) = c_{Ge}c_{Ge}S^{FZ}_{GeGe}(k) + c_{Se}c_{Se}S^{FZ}_{SeSe}(k) + 2c_{Ge}c_{Se}S^{FZ}_{GeSe}(k), \quad (1)$$

$$S_{NC}(k) = c_{Ge}c_{Se}\left[c_{Ge}\left(S^{FZ}_{GeGe}(k) - S^{FZ}_{GeSe}(k)\right) - c_{Se}\left(S^{FZ}_{SeSe}(k) - S^{FZ}_{GeSe}(k)\right)\right], \quad (2)$$

$$S_{CC}(k) = c_{Ge}c_{Se}\left\{1 + c_{Ge}c_{Se}\left[\left(S^{FZ}_{GeGe}(k) - S^{FZ}_{GeSe}(k)\right) + \left(S^{FZ}_{SeSe}(k) - S^{FZ}_{GeSe}(k)\right)\right]\right\}. \quad (3)$$

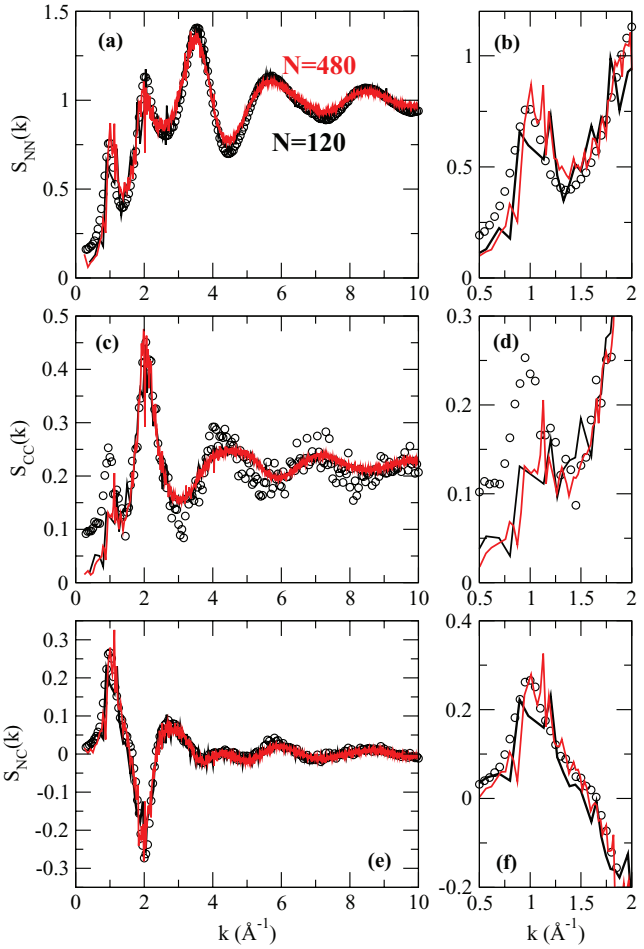

FIG. 1. The Bhatia-Thornton partial structure factors $S_{NN}(k)$ (top panels **a** and **b**), $S_{CC}(k)$, (middle panels **c** and **d**) and $S_{NC}(k)$ (bottom panels **e** and **f**) for liquid $GeSe_2$ at 1050 K. Results for the N = 120 (black line, Ref. 10) and N = 480 (red line) are compared to the experimental results of Ref. 1 (circles). The low wavevector regions for the three Bhatia-Thornton partial structure factors are highlighted in the panels **b**, **d**, and **f**.

Note that the calculated Faber-Ziman partial structure factors (not shown) differ only weakly with the system size, except in the FSDP region for $S^{FZ}_{GeGe}(k)$. Due to very close values of the coherent scattering length of the chemical species Ge and Se ($b_{Ge} = 8.185$ fm, $b_{Se} = 7.97$ fm)[44] and to the limited range of variation of $S_{NC}(k)$ and $S_{CC}(k)$, $S_{NN}(k)$ is a very good approximation of the total structure factor, i.e., $|S_T(k) - S_{NN}(k)| < 0.025$. Therefore, the considerations developed herafter on $S_{NN}(k)$ apply equally well to the total neutron structure factor $S_T(k)$.

The Bhatia-Thornton partial structure factors $S_{NN}(k)$ and $S_{NC}(k)$ perform better in the FSDP region for N = 480. Despite the presence of several spurious sub-peaks indicative of statistical noise and noticeable in $S_{NN}(k)$, the intensity of the feature seen at $k \sim 1$ Å^{-1} reaches the experimental one and is slightly higher in $S_{NC}(k)$. The overall shapes of $S_{NN}(k)$ and $S_{NC}(k)$ for larger values of k confirms the excellent agreement with experiments in this range of wavevectors (see Ref. 10). It is of interest to consider the behavior of $S_{CC}(k)$ due to the absence (or the large understimate) of the FSDP in the calculated $S_{CC}(k)$ for N = 120, strongly contrasting with the prominent feature found in neutron diffraction experiments.[1]

In the search of the origins of this disagreement, FPMD simulations of several liquids and glasses revealed that a sizeable FSDP was found to correspond to a small departure from chemical order, i.e., a moderate number of miscoordinations and homopolar bonds not severely affecting the tetrahedral-based network.[45,46] On the contrary, a FSDP in $S_{CC}(k)$ vanishes either when sufficiently higher levels of structural disorder set in, or, oppositely, when the chemical order is essentially perfect.[45,46] Accordingly, the FSDP in $S_{CC}(k)$ is absent in the simulation of liquid $GeSe_2$ due to a level of structural disorder comparatively much higher than in the experiment. Given these premises, the presence of a small peak in the FSDP region of $S_{CC}(k)$ for N = 480 (Fig. 1(d)) confirms that this specific feature is not adequately reproduced either for N = 120 or for N = 480.

IV. REAL SPACE PROPERTIES

A. Partial pair-correlation functions

Figure 2 provides a comparison between the two sets of calculations (for N = 120, Ref. 10 and N = 480) of the pair correlation functions $g_{GeGe}(r)$, $g_{GeSe}(r)$, and $g_{SeSe}(r)$, and the corresponding experimental results. Integration of the pair-correlation function $g_{GeSe}(r)$ over the first shell of neighbors leads to coordination numbers $\bar{n}_{GeSe}$ lying within 5% ($\bar{n}_{GeSe}$(exp) = 3.50, $\bar{n}_{GeSe}$ (N = 120) = 3.55, $\bar{n}_{GeSe}$(N = 480) = 3.66). In the case of $g_{SeSe}(r)$ the present value for $\bar{n}_{SeSe}$ is closer to the experimental one, i.e., $\bar{n}_{SeSe}$(exp) = 0.23, $\bar{n}_{SeSe}$(N = 120) = 0.33, $\bar{n}_{SeSe}$(N = 480) = 0.28. This allows to confirm the very good level of agreement previously found for $g_{GeSe}(r)$ and $g_{SeSe}(r)$ by employing a simulation cell with N = 120 atoms. The case of $g_{GeGe}(r)$ deserves some specific comments. For both system sizes, $g_{GeGe}(r)$ features a three peak structure at $r < 4$ Å, representative of homopolar bonds, edge-sharing, and corner-sharing connections. For N = 480, the first peak is similar in intensity to the experimental one, its width being clearly smaller. This has the effect of reducing the $\bar{n}_{GeGe}$(N = 480) coordination number to 0.14, to be compared with $\bar{n}_{GeGe}$ (N = 120) = 0.22 and $\bar{n}_{GeGe}$(exp) = 0.25. In the range 3 Å $< r <$ 4 Å, it appears that the shape of $g_{GeGe}(r)$ follows more closely the experimental one, the second and the third peak having closer intensities. However, the new set of data departs from the experimental trend and from the results at N = 120 in the range 6 Å $< r <$ 8 Å. This is an indication that the origin of the residual differences between theory and experiments is not necessarily the same for N = 480, as compared to the smaller size.

B. Coordination numbers and bond angle distributions

A clear insight into the network topology can be obtained through $n_\alpha(l)$. We define this quantity as the average number of atoms that are l-fold coordinated. For each coordination number (i.e., for each l) one can specify the identity of the first coordination shell, and establish the fraction of homopolar bonding. For instance, $GeSe_3$ (also termed Ge-$GeSe_3$ unit thereafter) with $l = 4$ (see Ge^{IV} plot in Fig. 3) means a fourfold coordinated Ge with one Ge and three Se

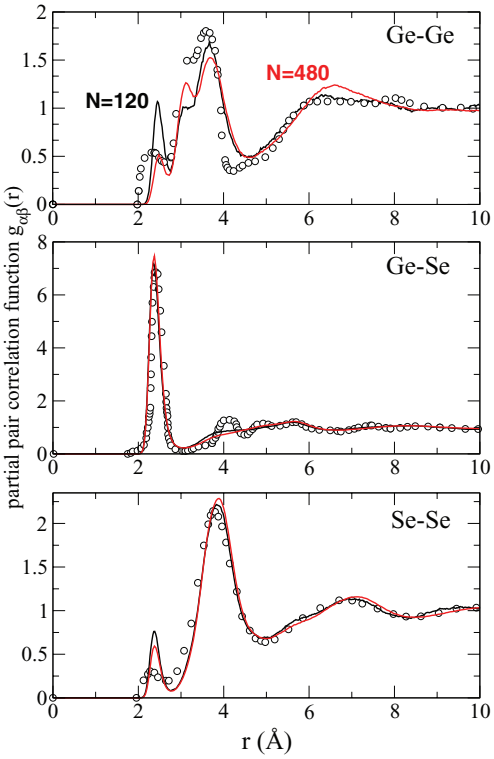

FIG. 2. The partial pair correlation functions $g_{GeGe}(r)$ (top panel), $g_{GeSe}(r)$ (middle panel) and $g_{SeSe}(r)$ (bottom panel) for liquid $GeSe_2$ at T = 1050 K. The results for N = 120 (black line, Ref. 10) and for N = 480 (present work, red line) are compared with the experimental results (circles, Ref. 1).

nearest-neighbors (i.e., one homopolar and three heteropolar bonds). Observation of the two panels on the leftmost side of Fig. 3 shows that the overall populations of Ge and Se atoms l-folded are quite similar for the N = 120 and the N = 480 cases. Referring to the fourfold Ge atoms, our results points toward close proportions of Ge-centered tetrahedra (respectively 65.1% and 65.6%). However, account of $n_\alpha(l)$ values reveals that the numbers of fully chemically ordered Ge tetrahedra and of twofold Se coordinated with two Ge atoms are larger for N = 480 (54.2% against 41.8% (case of Ge-Se_4 units) and 66.3% against 59.2%, (case of Se-Ge_2 units), respectively). This is an unambiguous sign of a size effect on the amount of the deviation from chemical order, that appears to be reduced when considering a larger system size. Indeed, the number of Ge and Se atoms miscoordinated is larger for N = 120, as it results from the larger percentages of Ge-Se_3, Ge-$GeSe_3$, Ge-$GeSe_4$, Se-GeSe, and Se-Ge_3.

In Fig. 4, we show for both system sizes the Se-Ge-Se (θ_{SeGeSe}) and Ge-Se-Ge (θ_{GeSeGe}) bond angle distributions. The identical and fully symmetrical shape of θ_{SeGeSe}

TABLE I. $E^{(k)}$ distribution (in %) in the liquid $GeSe_2$ for N = 120 and N = 480 atoms, as obtained from FPMD models.

	$E^{(0)}$	$E^{(1)}$	$E^{(2)}$
l-$GeSe_2$ (N = 120, Ref. 10)	61	34	5
l-$GeSe_2$ (N = 480, present work)	54	40	6
	N_{Ge}(ES)	N_{Ge}(CS)	$N_{Ge\text{-}Ge}$
l-$GeSe_2$ (N = 120, Ref. 10)	39	39	22
l-$GeSe_2$ (N = 480, present work)	46	40	14

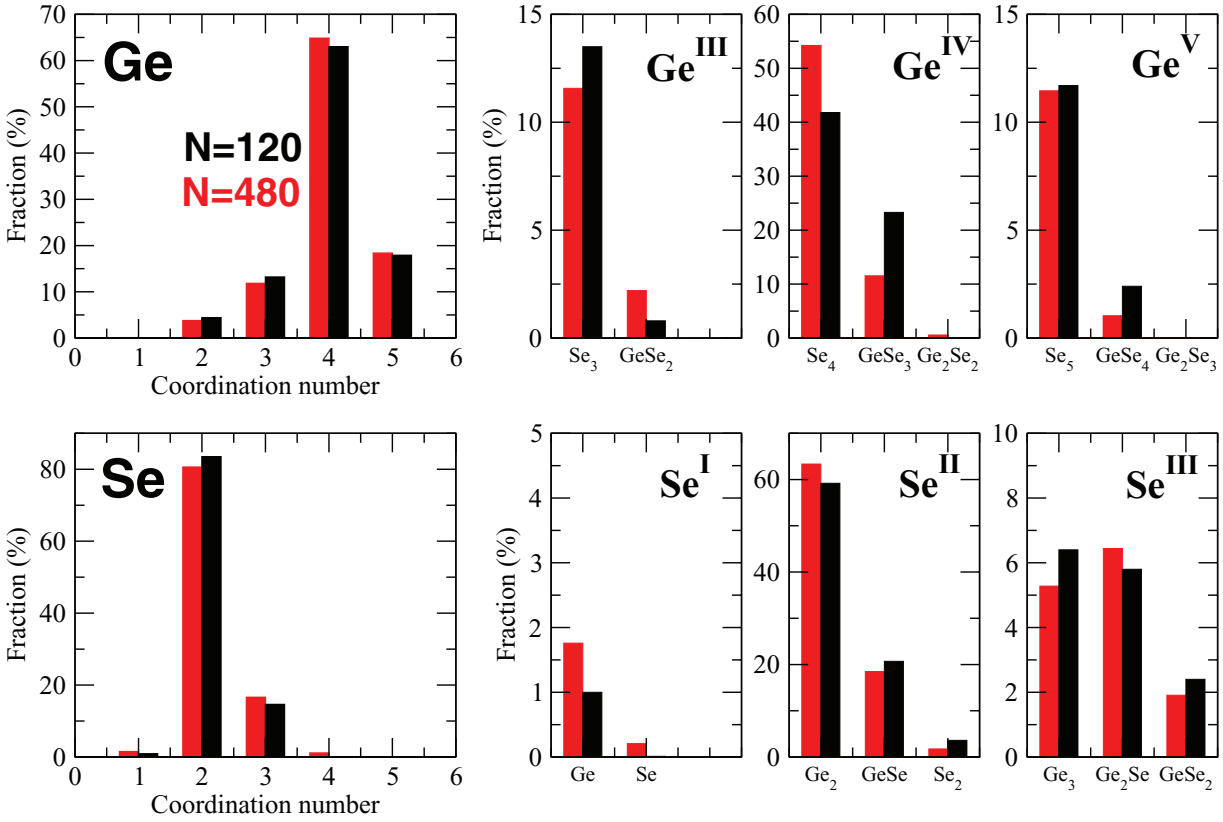

FIG. 3. Left column: The calculated population of l-fold coordinated Ge and Se atoms for N = 480 (red) and N = 120 (black, Ref. 10). Note that this population can be splitted into sub-populations Ge^{III}, Ge^{IV}, Ge^{V}, Se^{I}, Se^{II}, Se^{III}, providing information on the chemical nature of the first coordination shell (small panels on the right).

for the two cases is indicative of a predominant tetrahedral arrangement, with angles distributed around the expected value 109°. Therefore, the differences encountered in the chemical nature of the Ge-centered tetrahedra have no effect on θ_{SeGeSe}. As extensively detailed in previous papers, the two distinct peaks visible in the Ge-Se-Ge bond angle distribution at about 80° and 100° can be assigned to the formation of edge- and corner-sharing tetrahedra, respectively.[4,5,10] Changes in the egde-sharing/corner-sharing peak intensities ratio suggests that edge-sharing connections are more numerous for N = 480 than for N = 120. In order to obtain a quantitative assessment of this finding, we have resorted to the calculation of the number of Ge atoms that belong to zero, one, and two fourfold rings.

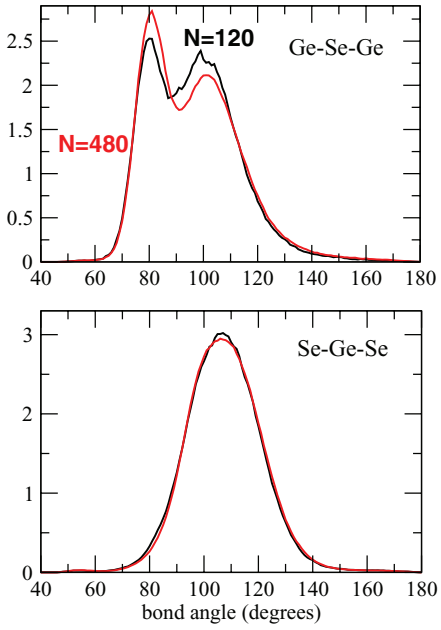

FIG. 4. The calculated bond-angle distributions θ_{GeSeGe} and θ_{SeGeSe} for liquid $GeSe_2$ at T = 1050 K. Black line: N = 120 (Ref. 10), red line : N = 480. These distributions have been calculated by including neighbors separated by less than 3 Å.

The algorithm used is based on the shortest-path criterion first proposed by King[47] and then improved by Franzblau.[48] Results are shown in Table I. According to such ring analysis, Ge atoms can be termed $E^{(0)}$ if they do not belong to any fourfold ring, $E^{(1)}$ if they are part of one fourfold ring, and $E^{(2)}$ if they belong to two fourfold rings.[49] As given in Table I, the larger system favors the presence of fourfold rings featuring the presence of one and two Ge atoms (46 for N = 480 against 39 for N = 120). From the values of $E^{(0)}$, $E^{(1)}$, and $E^{(2)}$, an estimate for the number of Ge atoms involved in corner sharing connections (N_{Ge}(CS)) can be obtained. To this end we adopted the proposal of Ref. 50, i.e., N_{Ge}(CS)= 1−N_{Ge}(ES)− $N_{Ge\text{-}Ge}$, which holds in the absence of extended chains.[50] By using the results quoted above (N = 480) and those given in Ref. 10 for N = 120 ($N_{Ge\text{-}Ge}$(N = 120) = 22%, $N_{Ge\text{-}Ge}$(N = 480) = 14%) one obtains that N_{Ge}(CS, N = 480) = 40%, N_{Ge}(CS, N = 120) = 39% leading to N_{Ge}(CS, N = 480)/N_{Ge}(ES, N = 480) = 0.87 and N_{Ge}(CS, N = 120)/N_{Ge}(ES, N = 120) = 1. This is consistent with

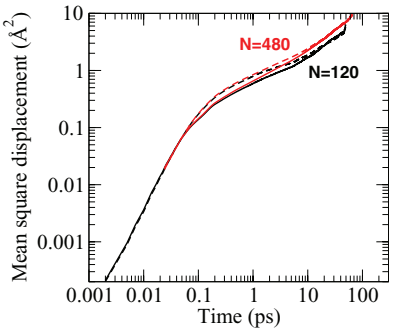

FIG. 5. Liquid $GeSe_2$ at 1050 K: mean square displacement (in Å^2) of Ge atoms (solid line) and Se atoms (broken line) for N = 480 (red line) and N = 120 (black line, Ref. 10).

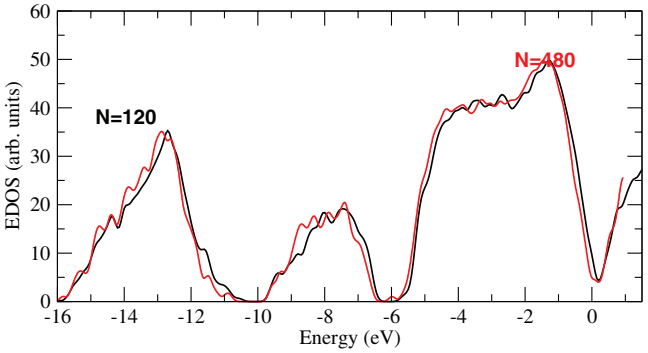

FIG. 6. The electronic density of states extracted from the Kohn-Sham eigenvalues. The result for the N = 120 liquid $GeSe_2$ (black line) is compared with that obtained for the N = 480 liquid $GeSe_2$ (red line). A Gaussian broadening of 0.1 eV has been employed.

the experimental prediction of Ref. 1, where the number of edge-sharing and corner-sharing sites were found very close. Therefore, both calculations for N = 120 and N = 480 confirm that the current theoretical scheme based on the BLYP XC functional is suitable to yield the correct relative proportion of corner-sharing and edge-sharing tetrahedra.

V. CORRELATION WITH DIFFUSION BEHAVIOR AND ELECTRONIC PROPERTIES

A. Mean-square displacement and diffusion constants

It is of interest to pursue the comparison between properties pertaining to the N = 120 and the N = 480 systems by accounting for the diffusion coefficient. We recall that the statistical average of the mean square displacement of chemical species α is given by

$$\left\langle r_\alpha^2(t)\right\rangle = \frac{1}{N_\alpha}\left\langle \sum_{i=1}^{N_\alpha} |\mathbf{r}_{i\alpha}(t) - \mathbf{r}_{i\alpha}(0)|^2 \right\rangle, \tag{4}$$

where $\mathbf{r}_{i\alpha}(t)$ is the coordinate of the ith particle of chemical species α at time t and N_α is the total number of particles of type α. The mean square displacements calculated for the Ge and Se atoms are shown in Fig. 5. The diffusive regime is reached in the long-time limit featuring a linear behaviour of $\log\langle r_\alpha^2(t)\rangle$ with $\log t$. Accordingly, the diffusion coefficient is then given by

$$D_\alpha = \frac{\left\langle r_\alpha^2(t)\right\rangle}{6t}, \tag{5}$$

The diffusion coefficients D_{Ge} and D_{Se} are given in Table II. These values are essentially identical, proving that the dynamical behavior is insensitive to the differences found in the chemical identity of the neighbors tetrahedrally coordinated to Ge atoms. As detailed in Refs. 10 and 51, calculated diffusion coefficients are consistent with the experimental result extracted from viscosity measurements,[52] i.e., $D_{\alpha,\,exp} = 0.045\times10^{-5}$ cm$^2 s^{-1}$/s.

TABLE II. The diffusion coefficients of the Ge and Se atoms in the liquid $GeSe_2$ for N = 120 (Ref. 10) and N = 480 atoms, as obtained from FPMD models.

	D_α ($\times 10^{-5}$ cm^2/s)	
	Ge	**Se**
l-$GeSe_2$ (N = 120, Ref. 10)	0.20	0.20
l-$GeSe_2$ (N = 480, present work)	0.20	0.19

On the basis of the above pieces of evidence, the question arises on the impact of the system size on the overall bonding character of liquid $GeSe_2$. Given the close coordination features and the persistent predominance of a (moderately defective) tetrahedral network, one does not expect drastic changes in the electronic properties, as exhibited at the level of the electronic density of states (EDOS). This is exactly what can be seen in Figure 6, in which the two EDOS appear very similar, both characterized by a marked pseudogap at the Fermi level.

VI. CONCLUSION

First-principles molecular dynamics calculations of the structural properties of liquid $GeSe_2$ have been undertaken on a periodic system four times larger (in terms of number of atoms, N = 480 against N = 120) than the one employed successfully in the past. Our main purpose was to achieve an insight on the possible occurrence of size effects, this issue deserving special attention due to the impact of extended (intermediate range) correlations in this kind of prototypical network. We found that the results for N = 480 do not alter the essence of what published in the case of N = 120, thereby confirming that N = 120 is an adequate size to capture most of the structural features. Nevertheless, a few moderate changes and/or improvements are worth pointing out. In real space, the short-range order is characterized by a higher degree of chemical order, with a larger number of Ge tetrahedra coordinated to four Se atoms. The tendency to reduce the deviation from chemical order has essentially no effect on either the diffusion coefficients or the electronic density of states. The present results suggest that, at least for liquid $GeSe_2$, size effects are not important when moving from ∼100 up to ∼500 atoms, calling for simulations on even larger systems to settle this issue in a conclusive manner. However, in the search of further quantitative improvements, a valuable alternative consists in adopting refined recipes for the exchange-correlations

functionals, provided these schemes can be coupled to efficient algorithms scaling linearly with the system size.[53–56]

ACKNOWLEDGMENTS

This work has been supported by the Agence Nationale de la Recherche (ANR) (Grant No. 09-BLAN-0109-01). Calculations were performed by exploiting resources allocated by the GENCI french national computer centers.

[1] I. T. Penfold and P. S. Salmon, Phys. Rev. Lett. **67**, 97 (1991).
[2] I. Petri, P. S. Salmon, and H. E. Fischer, Phys. Rev. Lett. **84**, 2413 (2000).
[3] H. E. Fischer, A. C. Barnes, and P. S. Salmon, Rep. Prog. Phys. **69**, 233 (2006).
[4] C. Massobrio, A. Pasquarello, and R. Car, Phys. Rev. B **64**, 144205 (2001).
[5] C. Massobrio and A. Pasquarello, Phys. Rev. B **77**, 144207 (2008).
[6] P. Biswas, D. N. Tafen, and D. A. Drabold, Phys. Rev. B **71**, 054204 (2005).
[7] D. N. Tafen and D. A. Drabold, Phys. Rev. B **71**, 054206 (2005).
[8] J. C. Mauro and A. K. Varshneya, J. Am. Ceram. Soc. **89**, 2323 (2006).
[9] C. Massobrio, A. Pasquarello, and R. Car, J. Am. Chem. Soc. **121**, 2943 (1999).
[10] M. Micoulaut, R. Vuilleumier, and C. Massobrio, Phys. Rev. B **79**, 214205 (2009).
[11] J. P. Perdew and Y. Wang, Phys. Rev. B **45**, 13244 (1992).
[12] A. D. Becke, Phys. Rev. A **38**, 3098 (1988).
[13] C. Lee, W. Yang, and R. G. Parr, Phys. Rev. B **37**, 785 (1988).
[14] C. Massobrio, P. S. Salmon, and M. Micoulaut, Solid St. Sci. **12**, 199 (2010).
[15] A. B. Bhatia and D. E. Thornton, Phys. Rev. B **2**, 3004 (1970).
[16] M. J. Haye, C. Massobrio, A. Pasquarello, A. De Vita, S. W. de Leeuw, and R. Car, Phys. Rev. B **58**, R14661 (1998).
[17] C. Massobrio, M. Celino, P. S. Salmon, R. A. Martin, M. Micoulaut, and A. Pasquarello, Phys. Rev. B **79**, 174201 (2009).
[18] S. Le Roux, A. Zeidler, P. S. Salmon, M. Boero, M. Micoulaut, and C. Massobrio, Phys. Rev. B **84**, 134203 (2011).
[19] M. Bauchy, M. Micoulaut, M. Celino, M. Boero, S. Le Roux, and C. Massobrio, Phys. Rev. B **83**, 054201 (2011).
[20] M. J. Mandell, J. Stat. Phys. **15**, 299 (1976).
[21] L. R. Pratt and S. W. Haan, J. Chem. Phys. **74**, 1864 (1981).
[22] A. R. Denton and P. A. Egelstaff, Z. Phys. B **103**, 343 (1997).
[23] L. Verlet, Phys. Rev. **159**, 98 (1967).
[24] S. M. Foiles, N. W. Ashcroft, and L. Reatto, J. Chem. Phys. **81**, 6140 (1984).
[25] L. Reatto and M. Tau, J. Chem. Phys. **86**, 6174 (1987).
[26] M. Rovere, D. W. Heermann, and K. Binder, Europhys. Lett. **6**, 585 (1988).
[27] D. P. Sellan, E. S. Landry, J. E. Turney, A. J. H. McGaughey, and C. H. Amon, Phys. Rev. B **81**, 214305 (2010).
[28] M. J. Mandell, J. P. McTague, and A. Rahman, J. Chem. Phys. **66**, 3070 (1977).
[29] J. N. Cape, J. L. Finney, and L. I. Woodcock, J. Chem. Phys. **75**, 2366 (1981).
[30] N. Choudhury and S. K. Ghosh, Phys. Rev. E **66**, 021206 (2002).
[31] F. Delogu, Phys. Rev. B **79**, 184109 (2009).
[32] S. S. Jang, R. W. Benz, S. H. White, and D. J. Tobias, J. Phys. Chem. B **110**, 7992 (2006).
[33] M. H. Müser and K. Binder, Phys. Chem. Miner. **28**, 746 (2001).
[34] J. J. Salacuse, A. R. Denton, and P. A. Egelstaff, Phys. Rev. E **53**, 2382 (1996).
[35] J. J. Salacuse, A. R. Denton, P. A. Egelstaff, M. Tau, and L. Reatto, Phys. Rev. E **53**, 2390 (1996).
[36] J. Ruska and H. Thurn, J. Non-Cryst. Solids **22**, 277 (1976).
[37] R. Car and M. Parrinello, Phys. Rev. Lett. **55**, 2471 (1985).
[38] N. Trouillier and J. L. Martins, Phys. Rev. B **43**, 1993 (1991).
[39] S. Nosé, Mol. Phys. **52**, 255 (1984).
[40] W. G. Hoover, Phys. Rev. A **31**, 1695 (1985).
[41] P. E. Blöchl and M. Parrinello, Phys. Rev. B **45**, 9413 (1992).
[42] J. C. Mauro and A. K. Varshneya, J. Am. Ceram. Soc. **90**, 192 (2007).
[43] D. Marx and J. Hutter, *Ab Initio Molecular Dynamics: Theory and Implementation*, in *Modern Methods and Algorithms of Quantum Chemistry*, J. Grotendorst ed. (NIC, FZ Jlich, 2000).
[44] P. S. Salmon, J. Non-Cryst. Solids **353**, 2959 (2007).
[45] C. Massobrio and A. Pasquarello, Phys. Rev. B **68**, 020201(R) (2003).
[46] C. Massobrio, M. Celino, and A. Pasquarello, Phys. Rev. B **70**, 174202 (2004).
[47] S. V. King, Nature (London) **213**, 1112 (1967).
[48] D. S. Franzblau, Phys. Rev. B **44**, 4925 (1991).
[49] M. Micoulaut, Physica B **212**, 43 (1995).
[50] I. Petri and P. S. Salmon, J. Phys. Condens. Matter **15**, S1509 (2003).
[51] M. Micoulaut and C. Massobrio, J. Optoelectron. Adv. Mater. **11**, 1907 (2009).
[52] S. Stolen, T. Grande, and H.-B. Johnsen, Phys. Chem. Chem. Phys. **4**, 3396 (2002).
[53] A. D. Becke, J. Chem. Phys. **98**, 5648 (1993).
[54] J. Heyd, G. E. Scuseria, and M. Ernzerhof, J. Chem. Phys. **118**, 8207 (2003).
[55] J. Heyd and G. E. Scuseria, J. Chem. Phys. **121**, 1187 (2004).
[56] J. VandeVondele, M. Krack, F. Mohamed, M. Parrinello, T. Chassaing, and J. Hutter, Comput. Phys. Commun. **167**, 103 (2005).